Spin absorption, windmill, and magneto-optic effects in optical angular momentum transfer

Davide Normanno, Marco Capitanio, and Francesco Saverio Pavone*
LENS, Università degli Studi di Firenze, Via N. Carrara 1,
I-50019 Sesto Fiorentino (FI), Italy INFM sez. Firenze, Via Sansone 1, I-50019 Sesto Fiorentino (FI), Italy
(Received 14 November 2003; published 30 November 2004)

Laser beams exert torque on microparticles through very different physical mechanisms. In this paper, optical angular momentum transferred by laser light to a trapped absorbing superparamagnetic microsphere has been studied, distinguishing between different contributions. We have found the main contribution to the torque arising from the transfer of the spin angular momentum carried by absorbed laser light. Detailed polarization status contribution of the laser light to the momentum transfer has been then analyzed. A general method to separate and quantify contributions to the optical angular momentum transferred has been developed. We have thus quantified contributions due to radiation pressure, through an effect similar to the wind on a windmill, and contributions arising from magneto-optic effects.

DOI: 10.1103/PhysRevA.70.053829 PACS number(s): 42.50.Nn, 42.25.−p, 87.80.Cc, 87.80.Fe

I. INTRODUCTION

The first theoretical calculation of the angular momentum exhibited by an elliptically polarized electromagnetic wave was done during the early years of the 1900s by Sadowsky and Epstein (whose works are noted in Ref. [2]). In 1909, Poynting [1] suggested an experiment devoted to showing that circularly polarized light would exert torque on a cascaded array of quarter-wave plates. However, the first experimental observation of optical angular momentum transfer only came 30 years later, when, in 1936, Beth [2] measured a feeble torque exerted on a doubly refracting plate suspended on a torsional pendulum, due to changes in the polarization of the transmitted light. An analogous experiment was performed in 1949 by Carrara [3], who used centimeter waves to measure both the torque due to absorption of elliptically polarized light and that due to photons scattering in different spin states. In 1966, Allen [4] showed that the torque transferred by circularly polarized radiation increases linearly with the light intensity. In recent years, the light-induced torque has been widely investigated in optical tweezers [5] where the angular momentum carried by the laser light is transferred to the trapped particle. The angular momentum carried by laser light exists in two distinct forms [6], namely the spin angular momentum, associated with the polarization of the beam [7], and the orbital angular momentum, associated with the spatial distribution of the beam [8]. Experiments were performed on the transfer of spin angular momentum due both to photon absorption [9,10] and to changes in the polarization of the transmitted beam caused by the birefringence of the trapped particle [11–13]. The transfer of orbital angular momentum was investigated in Refs. [14] and [15] using beams with a helical phase structure, while in Ref. [16] the transfer of orbital angular momentum was induced by an asymmetric beam shape to an asymmetric particle. Optical radiation can exert torque on asymmetric particles also through radiation pressure. Such an effect has been observed on interplanetary dust particles [17] and on micromachines trapped and rotated by laser light [18,19]. Radiation pressure on asymmetric particles resembles very much the effect of the wind on a windmill and is therefore called the "windmill effect." Furthermore, the light-induced torque is the basis of many optical devices [20–22], which have been developed to control rotations of microscopic objects for different applications among with microrheology [23] or biophysics studies.

In a recent paper [24], we have demonstrated a method to directly measure with pNnm sensitivity the torque exerted by the laser light on a trapped superparamagnetic microsphere.

The torque exerted by laser light on a trapped particle is usually transferred by different physical mechanisms. In this paper, we have investigated possible contributions to the light-induced torque, which have been now quantified and properly separated. In particular, we have investigated the laser polarization status in order to understand the spin angular momentum carried by the laser light. We have developed a method to separate and quantify contributions to the transferred torque related to not perfectly spherical shaped or inhomogeneous beads, arising from the radiation pressure (windmill effect). We have also quantified contributions due to magneto-optic effects [25], arising from the passage of the laser light through a magnetized (thus birefringent [25]) bead. Finally, we have discussed the interaction between superparamagnetic beads and a magnetic homogeneous field, such as the one applied by our magnetic manipulator.

II. LASER BEAM POLARIZATION

In order to measure the optical angular momentum transfer, we used a custom magneto-optic manipulator, developed by our group [26–28], constituted by an optical tweezers setup integrated with a magnetic manipulator. The optical tweezers allow trapping of superparamagnetic microspheres while, at the same time, the magnetic manipulator offers the possibility of bead rotations. Furthermore, using an interferometric detection scheme, based on differential interference contrast (DIC) microscopy [29], we detect rotations of

*Corresponding author. Email address: pavone@lens.unifi.it

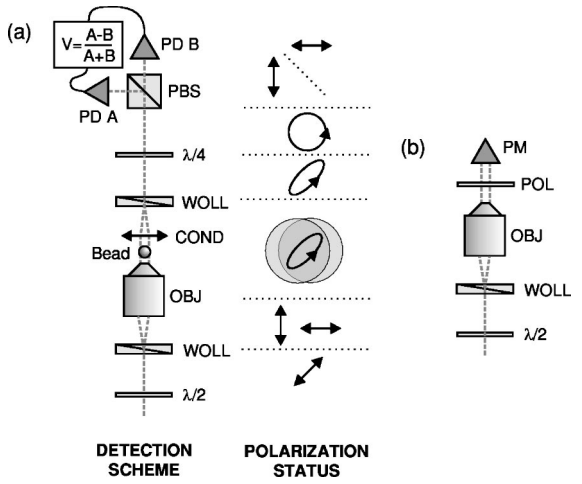

FIG. 1. (a) The interferometric detection scheme (DIC) and the polarization status of the trapping light. WOLL is a Wollaston prism, OBJ is the microscope objective, COND is the microscope condenser, PBS is a polarizing beam splitter, and PD A and PD B are two identical photodiodes. (b) The scheme used to measure the polarization ellipticity in the trapping region. POL is a polarizer and PM is a power meter. The ellipticity was obtained by rotating the polarizer and measuring the ratio between the minimum and the maximum laser power. The polarization angle was varied by means of the $\lambda/2$ waveplate.

slightly asymmetrical beads. In the DIC detection scheme [Fig. 1(a)], the first Wollaston prism angularly separates the infrared laser light (from a Nd:YAG emitting at 1064 nm) in two beams with orthogonal polarizations. The beams are focalized by the objective to two diffraction limited and overlapped spots, where trapping occurs, and are finally recombined after the condenser by the second Wollaston prism. The $\lambda/4$ waveplate transforms the polarization to circular when the bead is in the center of the trap; a bead movement or rotation (on slightly asymmetrical beads) changes the beam polarization and is measured by the signal V.

The first Wollaston prism, designed to work with visible light, induces a phase shift between the two outcoming beams and in the trapping region the polarization becomes elliptical [see Fig. 1(a)].

The polarization ellipticity, defined as the ratio between the minor and the major axes of the polarization ellipse, has been measured after the objective in order to investigate the behavior of the polarization in the trapping region. The polarization angle of the beam entering in the first Wollaston prism was varied by means of a $\lambda/2$ waveplate, and the corresponding polarization ellipticity in the trapping region was then measured using a polarizer and a power meter [see Fig. 1(b)].

The measured polarization ellipticity in the trapping region [see Fig. 2(a)] can be accounted for by a constant phase shift $\varphi \sim 0.31$ rad between the two outcoming beams, induced by the first Wollaston prism.

A monochromatic beam with an arbitrary elliptical polarization $\boldsymbol{E}=E_{0x}e^{-i\omega t}\boldsymbol{i}+E_{0y}e^{i\varphi}e^{-i\omega t}\boldsymbol{j}$ in the paraxial approximation carries a spin angular momentum $\boldsymbol{\Gamma}^{\sigma}=1/\omega\int dxdyIs_3=P^{\sigma}/\omega$, where I is the light intensity, $s_3=2E_{0x}E_{0y}\sin\varphi/(E_{0x}^2+E_{0y}^2)$, and P^{σ} is the fraction of laser power carrying spin angular momentum [30]. Assuming a constant intensity profile beam, we have calculated the spin angular momentum carried by the trapping light as shown in Fig. 2(b). The maximum value of the spin angular momentum corresponds to an angle $\varphi_{\lambda/2}\approx 45°$ between the laser polarization and one of the principal axes of the Wollaston prism. This is also the standard configuration for the DIC detection when the two outcoming beams have equal intensities and corresponds to a spin angular momentum of about 170 pNnm/mW. This is the only component of the carried angular momentum, because the laser beam is a TEM_{00} Gaussian mode, which does not transport orbital angular momentum. When trapped, we typically observed beads slowly rotating in a counterclockwise sense; we expect that the transferred torque arises from the transfer of spin angular momentum carried by the laser light due to absorption, because superparamagnetic beads absorb a small portion of the laser light [24,28]. Nevertheless, sometimes superparamagnetic beads did not rotate and, in rare cases, we also observed beads rotating clockwise. We therefore expect that also other effects which depend on the single bead can contribute to the transferred torque.

III. MEASUREMENTS OF THE TRANSFERRED OPTICAL ANGULAR MOMENTUM

In Ref. [24], we developed a general method to measure the torque induced by laser light on superparamagnetic microbeads. Here, as shown throughout the paper, we will demonstrate how to separate and quantify the effects that contribute to the transferred torque. In our configuration, the transferred optical angular momentum $\boldsymbol{\Gamma}^{rad}$ may be addressed to several contributions. Because the bead is not perfectly spherical, such contributions can be divided into two classes:

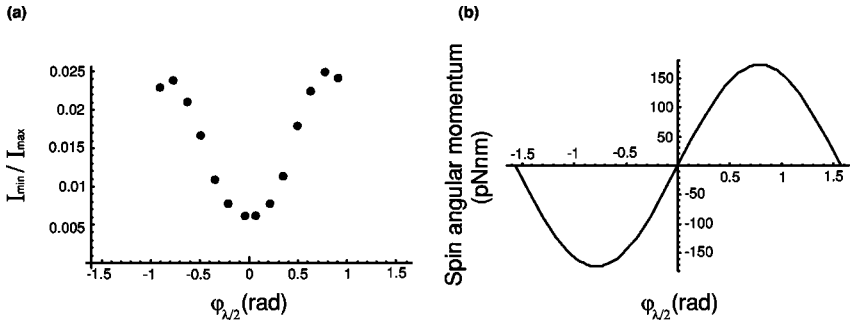

FIG. 2. (a) Measurements of the ratio between the intensities along the minor (I_{min}) and the major (I_{max}) axis of the polarization ellipse in the trapping region. $\varphi_{\lambda/2}$ is the angle between the light polarization and one of the principal axes of the Wollaston prism. (b) Calculation of the spin angular momentum $\boldsymbol{\Gamma}^{rad}$ carried by 1 mW of laser light in the trapping region.

$\tilde{\Gamma}^{rad}$, whose magnitude and sign depend on the orientation of the asymmetric particle with respect to a linearly polarized [22,31] or asymmetric [16] beam; $\overline{\Gamma}^{rad}$, which is independent of the orientation, like the spin angular momentum transferred due to absorption (Γ^{σ}), or a contribution arising from the windmill effect (Γ^{pr}). Thus,

$$\Gamma^{rad} = \tilde{\Gamma}^{rad} + \overline{\Gamma}^{rad} = \tilde{\Gamma}^{rad} + \Gamma^{\sigma} + \Gamma^{pr}. \quad (1)$$

Also, contributions related to magneto-optics effects may be present as discussed in Sec. V.

Using our magneto-optic manipulator, we rotate a trapped bead with a rotational drag coefficient γ and angular velocity ω. The bead experiences a drag torque $\Gamma^{drag} = -\gamma\omega$, a torque Γ^{mag} due to the magnetic manipulator, and a torque Γ^{rad} due to the laser light. Γ^{mag} can be measured from the phase shift $\Delta\phi$ between the bead rotation signal and the magnetic field rotation signal as $\Gamma^{mag} = -k_{rot}(|\Delta\phi| - \Delta\phi_0)\hat{z}$, where k_{rot} is the torsional stiffness of the magnetic manipulator, $\hat{z}$ is the unit vector along the vertical axis, and $\Delta\phi_0$ is the limit of $|\Delta\phi|$ when the external torque applied to the bead goes to zero (see Ref. [24] and the Appendix for a discussion about the interaction between the magnetic field applied by the magnetic manipulator and a superparamagnetic bead). We can measure Γ^{rad}, distinguishing between the contribution due to $\overline{\Gamma}^{rad}$ from that due to $\tilde{\Gamma}^{rad}$, by rotating the bead clockwise (CW) and then counterclockwise (CCW). Γ^{drag} and Γ^{mag} change sign between CW and CCW rotations as does $\tilde{\Gamma}^{rad}$, while $\overline{\Gamma}^{rad}$ does not. Thus, from the difference between the two measurements, we obtain $\overline{\Gamma}^{rad}$ [24], and from the sum between the two measurements one can quantify $\tilde{\Gamma}^{rad}$.

The phase shift $\Delta\phi$ in the steady state is given by

$$\Delta\phi^{CW,CCW}(\omega) = \frac{\gamma}{k_{rot}}|\omega| \pm \left(\frac{\overline{\Gamma}^{rad}}{k_{rot}} + \Delta\phi_0\right) + \frac{\tilde{\Gamma}^{rad}}{k_{rot}} = a|\omega| + b^{CW,CCW}, \quad (2)$$

where the signs + and − refer correspondingly to CW and CCW rotation.

From Eq. (2), we are able to determine the values of $\tilde{\Gamma}^{rad}$ and $\overline{\Gamma}^{rad}$, respectively, from the sum and the difference of the values of the intercepts b^{CW} and b^{CCW},

$$\tilde{\Gamma}^{rad} = \frac{1}{2}k_{rot}(b^{CW} + b^{CCW}),$$

$$\overline{\Gamma}^{rad} = \Gamma^{\sigma} + \Gamma^{pr} = \frac{1}{2}k_{rot}(b^{CW} - b^{CCW} - 2\Delta\phi_o). \quad (3)$$

Furthermore, from Eq. (2) we also obtain the torsional stiffness $k_{rot} = \gamma/a$ of the magnetic manipulator.

Figure 3 shows the behavior of $\overline{\Gamma}^{rad}$ and $\tilde{\Gamma}^{rad}$ as a function of laser power in a typical experiment. $\overline{\Gamma}^{rad}$ behaves linearly with the laser power and goes to zero when the laser power goes to zero. The linear fit gives a value of the slope of 9.5 ± 0.7 pNnm/mW. On the other hand, the $\tilde{\Gamma}^{rad}$ value is distributed, within the experimental error, around a null

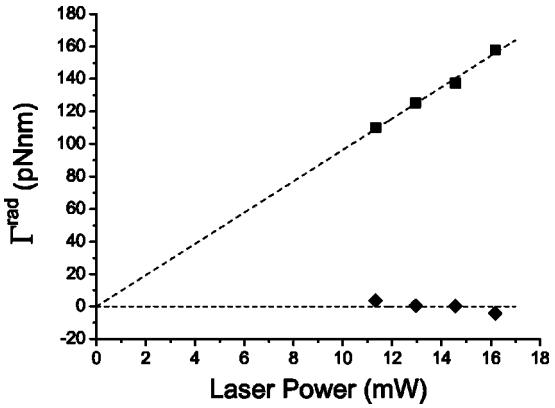

FIG. 3. The transferred angular moment $\overline{\Gamma}^{rad}$ (■) and $\tilde{\Gamma}^{rad}$ (◆) vs laser power on the sample.

value. This behavior can be explained taking into consideration that the torque contribution $\tilde{\Gamma}^{rad}$ is null in our case because this effect, even if it were not negligible, is averaged on an integer number of turns and so has a null average value. In any case, with this method it is possible to separate and quantify possible systematic contribution to the torque.

All the experiments were performed with (2.6 ± 0.1) μm -diam beads positioned about 30 μm inside the sample cell. Within the apparatus sensitivity ($\sim$ pNnm), we did not observe any differences in k_{rot} when rotating CW or CCW, which means that, despite the bead asymmetry, γ is equal for CW and CCW rotations. Again, we did not observed any dependence of k_{rot} with laser power, which means that, despite the bead absorbance, the induced magnetic dipole does not depend on the bead temperature.

IV. SEPARATION OF THE SPIN ANGULAR MOMENTUM AND THE WINDMILL EFFECT

In order to properly quantify and separate the different contributions to the optical angular momentum transfer that appear in Eq. (1), we used the experimental configuration depicted in Fig. 4(a). We removed the DIC optics and placed a $\lambda/4$ waveplate in the beam path before the objective; in this way, the polarization of the beam could be regulated between left (σ_+) and right (σ_-) circularly polarized. Again, we observed the beads rotating CCW or CW, depending on the polarization σ_+ or σ_-. The bead rotation was detected by means of a quadrant detector photodiode (QDP) placed in the back focal plane of the condenser. We found the QDP able to directly measure the angle α formed by a slightly asymmetrical bead with respect to a reference axis [see Fig. 4(b)]. In fact, the X(t) and Y(t) signals coming from the QDP are, respectively, proportional to $\cos[\alpha(t)]$ and $\sin[\alpha(t)]$, and the α angle can then be measured as $\alpha(t) = \arctan[Y(t)/X(t)]$. The X(t) and Y(t) signals were averaged on a running window 50 points wide using a sampling rate of 1 kHz. Depending on the polarization σ_+ or σ_-, $\alpha(t)$ varied between $-\pi/2$ and $+\pi/2$ with a constant positive or negative slope. From the sign of $d\alpha/dt$, we distinguished the rotation direction, and from the FFT of $\alpha(t)$ we obtained ω. Neglecting $\tilde{\Gamma}^{rad}$

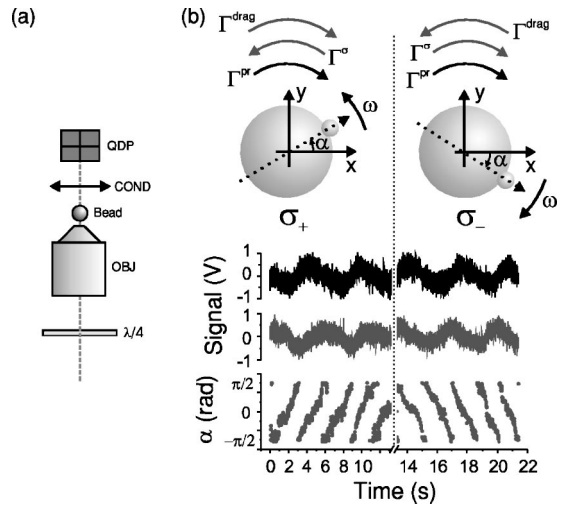

FIG. 4. (a) The scheme utilized to separate the contribution to the transferred torque due to photon spin and to radiation pressure. (b) In the upper part of the figure, the different contributions of the torque applied to the bead are represented for left circularly polarized (σ_+) and right circularly polarized (σ_-) light. The small bead represents the bead asymmetry. In the lower part of the figure, the X(t) and Y(t) signals come from the QDP (black and gray lines, respectively), and the α angle, measured as $\alpha(t) = \arctan[Y(t)/X(t)]$.

because of its null average value, the steady-state condition is $\Gamma^{rad} = \Gamma^{drag} = \gamma\omega$ and the optical angular momentum transferred can be obtained from the bead rotation frequency. Measurements of Γ^{rad} versus light polarization, reported in Ref. [24], show that the transferred torque follows the polarization ellipticity of the laser light, which means that most of the transferred torque is due to spin angular momentum transfer caused by absorption. Besides this, we found an additional contribution to the torque, stronger on more asymmetric beads. In order to investigate this effect, we chose a fairly asymmetric bead and we measured Γ^{rad} versus laser power using pure left circularly polarized (σ_+) and right circularly polarized (σ_-) light (see Fig. 5).

Γ^{rad} clearly shows a linear dependence on laser power, but the linear fits depicted in Fig. 5 show two different slopes ($k^+ = 97 \pm 14$ pNnm/mW and $k^- = -25 \pm 3$ pNnm/mW for σ_+ and σ_-, respectively). Such a behavior provides evidence that Γ^{rad} is the sum of absorption-based spin angular momentum Γ^{σ} and of an angular momentum contribution Γ^{pr}, which both linearly depend on laser power P,

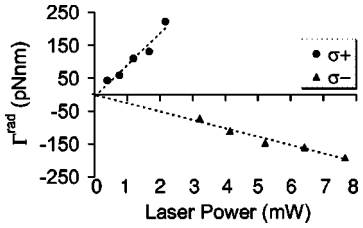

FIG. 5. Transferred torque vs laser power for σ_+ and σ_-.

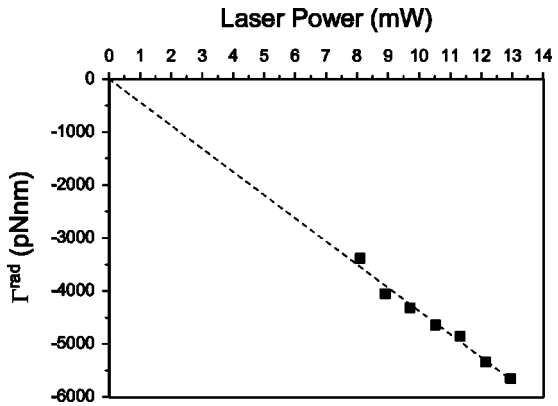

FIG. 6. Transferred torque vs laser power. In this case, the contribution due to the windmill effect is predominant. The linear fit gives a slope of -440 ± 25 pNnm/mW.

$$\Gamma_{\pm}^{rad} = \pm\Gamma^{\sigma} + \Gamma^{pr} = (\pm k^{\sigma} + k^{pr})P\hat{z} = k^{\pm}P\hat{z}, \tag{4}$$

where $+$ and $-$ refer to σ_+ and σ_-, and k^{σ}, k^{pr}, and $k^{\pm}$ are constants. The linear behavior and the dependence on the bead shape suggest that Γ^{pr} arises from radiation pressure, through the windmill effect. From Eq. (4), we obtain

$$k^{\sigma} = \frac{k^+ - k^-}{2}, \quad k^{pr} = \frac{k^+ + k^-}{2}. \tag{5}$$

Using Eq. (5), we have therefore separated and quantified k^{σ} and k^{pr} ($k^{\sigma} = 61 \pm 9$ pNnm/mW and $k^{pr} = 35 \pm 9$ pNnm/mW for the measurement reported in Fig. 5). The transferred torque due to the windmill effect is usually smaller or at most comparable with respect to the spin angular momentum transfer caused by absorption. However, it is worth noting that, in the case of extremely asymmetric beads or beads with big superficial impurities, the transferred torque related to the windmill effect may be even bigger than the spin contribution, as shown in Fig. 6. Here, despite the use of the magneto-optic manipulator, where Γ^{σ}, due to spin angular momentum transfer caused by absorption, is positive, the measured Γ^{rad} is negative, confirming that the windmill effect may in rare cases be the predominant effect.

V. MAGNETO-OPTIC EFFECTS MEASUREMENTS

The use of the magneto-optic manipulator introduces a further possible source of angular momentum transfer. In fact, the passage of the laser light through the magnetized (thus birefringent) bead induces changes in the polarization due to magneto-optic effects. Here, we have studied the polarization of both the transmitted and the reflected beam in order to complete the analysis of the contributions to the optical angular momentum transfer. In general, circular birefringence and dichroism (Faraday effect) appear on the transmitted beam when the wave number $\boldsymbol{k}$ is parallel to the magnetization $\boldsymbol{M}$, while linear birefringence and dichroism (Voigt effect) appear when $\boldsymbol{k}$ it is orthogonal to $\boldsymbol{M}$. The Kerr effect rotates the polarization and changes the polarization ellipticity of the reflected beam, and is more pronounced for $\boldsymbol{k}$ parallel to $\boldsymbol{M}$. Faraday and Kerr effects turn out to be

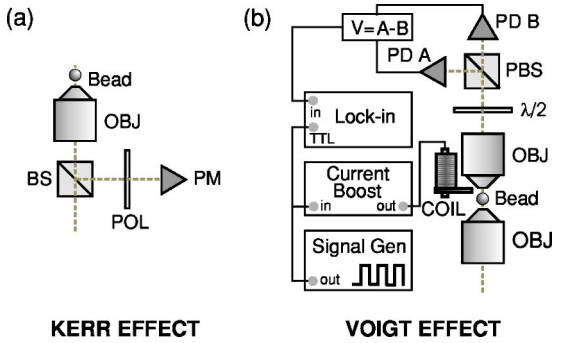

FIG. 7. (a) The scheme used to measure the variation of the reflected beam polarization. OBJ is the microscope objective, BS a 50% beam splitter cube, POL a polarizer, and PM a power meter. The scheme is analogous to that represented in Fig. 1(b). (b) The scheme used to measure the variation of the transmitted beam polarization. PBS is a polarizing beam splitter cube and PD A and PD B are two identical photodiodes.

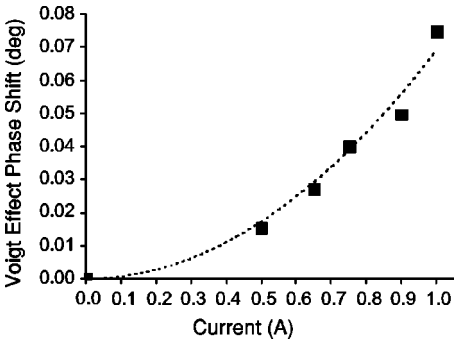

FIG. 8. The measured Voigt phase shift φ vs the boost current i. The angle between B and the light polarization was chosen in order to maximize the effect. Dotted line is the fitted theoretical prediction ($\varphi=\chi i^2$, which gives $\chi=1.2\mathrm{E}-3$ rad A^{-2}).

proportional to $\boldsymbol{M}$, while the Voigt effect is proportional to $|\boldsymbol{M}|^2$. In our configuration, Voigt birefringence should be predominant because (a) the beam travels orthogonal to $\boldsymbol{B}$ (and thus $\boldsymbol{M}$), (b) for symmetry reasons, Faraday and Kerr effects should be zero for a bead trapped by a TEM_{00} laser beam, (c) Faraday and Voigt dichroism acts only on the portion of light absorbed by the bead and Kerr effect on the reflected one.

Polarization changes on the reflected beam due to the magneto-optic Kerr effect were measured using the scheme depicted in Fig. 7(a). Here, a 50% beam splitter cube was used to select the back-reflected beam; a polarizer together with a power meter were used to measure the polarization ellipticity of the beam, when a zero and a 48-G magnetic field was applied in various directions. We found that the ellipticity was constant within the measurement sensitivity (0.06). Considering the measured reflected power (0.2%), an upper limit on the Kerr-induced torque of 0.2 pNnm/mW was evaluated, which is negligible compared to that induced by photons absorption.

In order to probe changes in the polarization of the transmitted beam with higher sensitivity, we used the scheme represented in Fig. 7(b). Here, analogously to the DIC detection, the signal V is sensitive to polarization changes. A second objective [numerical aperture (NA) of 1.4] was utilized in order to collect all the transmitted light, and the $\lambda/2$ waveplate was rotated in order to set V to zero when a bead was trapped and no magnetic field was applied. The amplitude of the magnetic field was modulated, from 0 to 48 Gauss, driving the electromagnet coils with a square-modulated current signal from 0 to 2 A at 275 Hz, and a lock-in amplifier was used for synchronous detection.

As discussed above, we assume that only the Voigt linear birefringence is present. In this case, we can, for small phase shifts, relate unequivocally the signal V with the Voigt phase shift. We found that the phase shift had an even dependence in the $\boldsymbol{B}$ direction, and behaved as $|\boldsymbol{B}|^2$, as expected for the Voigt effect, thus confirming our assumption (Fig. 8). From the measured phase shift, a maximum angular momentum transferred to the bead of 0.4 pNnm/mW was derived, negligible again when compared to the one induced by photons absorption.

VI. CONCLUSION

In this paper, we measured the torque exerted by an elliptically polarized laser beam on a superparamagnetic bead, evidencing different contributions such as spin angular momentum transfer caused by absorption and by magneto-optic effects, and torque induced by radiation pressure through the windmill effect.

We have developed a method to separate and quantify these different contributions, whose order of magnitude and cause are summarized in Table I. We have demonstrated that, in most cases, the main contribution to the torque is related to the transfer of spin angular momentum due to absorption. The windmill effect is related to the not perfect spherical shape of the bead; it depends on the single bead and usually turns out to be smaller (less than 20%) with respect to the spin angular momentum transfer. We have also investigated the magneto-optic effects, due to birefringence and dichroism in the transmitted beam (Faraday and Voigt effects), or caused by changes in the polarization of the reflected beam (Kerr effect). Measurements of polarization changes on both transmitted and reflected beams showed that magneto-optic effects exert a negligible torque (about 1%) with respect to the other contributions.

The capability of distinguishing the different contributions to the torque, and the high sensitivity of the apparatus,

TABLE I. Summary of the different contributions to the optical angular momentum transferred

Effect	Contribution (pNnm/mW)
Spin angular momentum exchanged by absorption	50–150 pNnm/mW for circularly polarized light
Windmill effect due to radiation pressure	Less than 25 pNnm/mW in most cases
Magneto-optic effects (Kerr, Voigt, and Faraday effects)	0.1–0.5 pNnm/mW

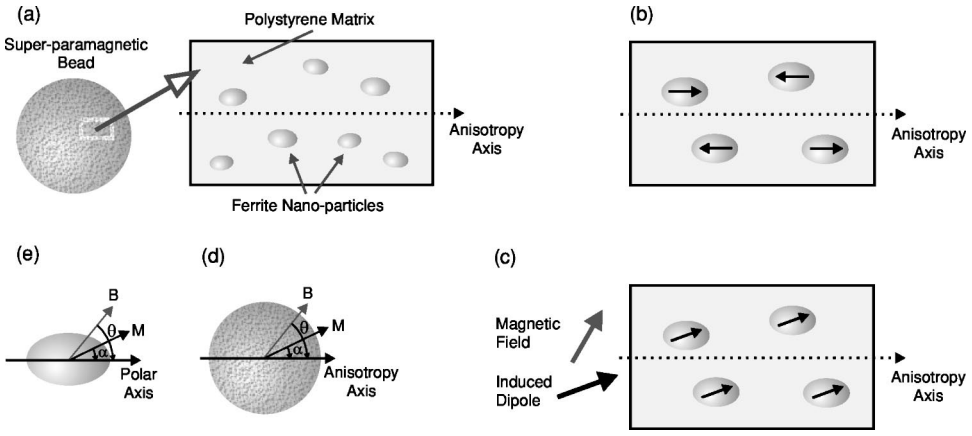

FIG. 9. (a) The behavior of superparamagnetic beads can be explained by assuming the presence of an anisotropy axis along which ferrite nanoparticles align. (b) In the absence of an external magnetic field, the two "easy" configurations are equally populated and the bead magnetic dipole is null. (c) In the presence of a magnetic field, an induced magnetic dipole is generated along a direction between the magnetic field and the anisotropy axis. (d) Definition of the angles for a single superparamagnetic bead. (e) Definition of the angles for a single ferrite nanoparticle.

combined with the use of functionalized microbeads, allow its use in biophysics applications. Here, the understanding of the light-induced torque on microbeads is crucial for the measurement of the torque exerted by polymers or biomolecules in single molecule assays. The magneto-optic manipulator could be, for example, utilized to directly measure the torsional stiffness of a single DNA molecule [32,33], or the torque exerted by a rotary motor [34]. In such an experiment, it will be important to take into account all the torque contributions arising from the trapping laser light.

ACKNOWLEDGMENTS

We thank Maurizio Artoni and David Sampson for advice and observations. We acknowledge Enrico Santamato and Angelo Rettori for useful consideration. This work was supported under Contract No. HPRI-CT-1999-00111 CE, and partially supported by the "SINPHYS" PAIS 2002 project of INFM.

APPENDIX: INTERACTION BETWEEN SUPERPARAMAGNETIC BEADS AND THE MAGNETIC FIELD

In order to better understand the torque measurements performed with the magneto-optic manipulator described in Sec. III, let us consider the interaction between a uniform magnetic field and a superparamagnetic bead.

Superparamagnetic beads are usually constituted by ferrite and/or maghemite nanoparticles dispersed in a matrix of polystyrene, obtained from styrene polymerization. In our experiments, we used BE-M08/26 streptavidin coated superparamagnetic beads, 2.6 μm diameter, 32.7% ferrite pigment content from Merck Eurolab (France). In order to obtain ferrite particles with superparamagnetic behavior, the particle dimensions are smaller than 30 nm, typically about 15 nm, with a mean interparticle displacement of about 50 nm [35]. At room temperature, the beads do not present any hysteresis [28,35,36], and, in this sense, they behave as truly paramagnetic. On the other hand, single spherical beads are put in rotation by a rotating magnetic field [27,28,35,37,38] (see the two included movies of two trapped and single beads rotated by a rotating magnetic field. The beads have been chosen with sufficient asymmetric shape in order to visualize the rotation [39].) When rotated, superparamagnetic beads behave as a permanent magnetic dipole, whereas the amplitude of the magnetic dipole linearly depends on the magnetic field for small magnetic fields [28]. Such a behavior could be explained if the internal ferrite structure had an asymmetric or anisotropic distribution. We have not found specific information on the internal structure of BE-M08/26 beads in the literature.

An asymmetric distribution of ferrite particles has been reported in the literature [40,41], and a theoretical analysis which justifies the torque applied by an external magnetic field can be found in Ref. [42]. In Ref. [42], the rotation of a chain of superparamagnetic beads has been observed when subject to an external rotating magnetic field; the applied torque is justified using a simple chain model in which dipole-dipole interaction tends to orient the magnetic dipoles parallel to the chain axis and to the external magnetic field. Considering the equilibrium between the hydrodynamic drag and the magnetic torque, a phase lag ϑ is theoretically and experimentally found between the magnetic field and the chain axis, which, for small angles, is proportional to the applied torque. In our case, an asymmetric distribution of ferrite particles inside the bead (or due to the asymmetric shape of the bead) would lead to a torque applied by an external field, which would tend to orient the bead along the asymmetry axis. The linear dependence of the applied torque with respect to the angle ϑ ($\Gamma^{mag}=-k_{rot}\vartheta$) can then be justified as in Ref. [42].

Even if the ferrite particles were randomly dispersed inside the polystyrene matrix [41,43], but with a preferred orientation along an "anisotropy" axis [Fig. 9(a)], the presence of a torque exerted by an external magnetic field could be justified. A preferred orientation could arise during bead for-

mation (polymerization) as a consequence of magnetic or electrostatic interactions between the ferrite nanoparticles, between the ferrite nanoparticles and an external field, or because of interactions between the ferrite particles and the polystyrene matrix. Under this assumption, in the absence of an external magnetic field, the bead magnetic dipole is null because, on average, the two "easy" configurations are equally populated [44] [see Fig. 9(b)]. In the presence of a magnetic field, an induced magnetic dipole is generated along a direction between the magnetic field and the anisotropy axis [Fig. 9(c)].

Experimental evidence accounts for a simple model in which thermal forces are dominated by magnetic and hydrodynamic forces. Let us assume that a single ferrite particle is a rotational ellipsoid oriented as in Fig. 9(e). The free energy of a single ferrite particle in the presence of a homogeneous magnetic field $\boldsymbol{B}$ is given by [44]

$$F_T = \frac{1}{2} CV \sin^2 \alpha - BMV \cos(\vartheta - \alpha), \tag{A1}$$

where C is the crystalline anisotropy constant, V is the particle volume, ϑ is the angle between $\boldsymbol{B}$ and the polar axis, and α is the angle between the magnetization vector $\boldsymbol{M}$ and the polar axis [Fig. 9(e)]. Under the assumption that all the ferrite particles are oriented along the same axis, that they have identical shape, volume, and intrinsic magnetic dipole, and that they do not interact between each other, we calculate the free energy of a superparamagnetic bead in the presence of a homogeneous magnetic field as

$$F = NF_T = N\left[\frac{1}{2} CV \sin^2 \alpha - BMV(\cos \vartheta \cos \alpha + \sin \vartheta \sin \alpha)\right], \tag{A2}$$

where N is the number of ferrite particles inside the bead. For a fixed ϑ, the free energy is obtained by equating to zero the derivative of Eq. (A2) with respect to α and assuming α small. The torque Γ^{mag} exerted by the magnetic field is then obtained by differentiating the free energy with respect to ϑ. For small ϑ,

$$\boldsymbol{\Gamma}^{mag} = -N\left\{BMV\left[1 + \frac{B^2M^2}{(C+BM)^2} - \frac{2BM}{C+BM}\right] + \frac{B^2CM^2V}{(C+BM)^2}\right\}\vartheta = -k_{rot}\vartheta. \tag{A3}$$

Equation (A3) shows a linear behavior of ϑ with respect to Γ^{mag}, as confirmed by experimental results [28]. For $C \ll 1$, $\Gamma^{mag} \approx 0$ and the bead behaves as truly paramagnetic, whereas for $C \gg 1$, $\Gamma^{mag} \approx -BMV\vartheta$ and the bead responds to torques as a permanent magnetic dipole.

We can therefore model the magnetic manipulator as a torsional spring attached to superparamagnetic beads. The applied torque is given by Eq. (A3), where ϑ is the angle between the applied magnetic field $\boldsymbol{B}$ and the anisotropy or asymmetry axis; we indicate this axis as $\boldsymbol{m}$, in order to recall the analogy with the interaction between a homogeneous magnetic field and a permanent magnetic dipole. Superparamagnetic beads can be rotated by rotating the magnetic field, and the ϑ angle can be measured from the phase shift between the bead rotation signal and the magnetic field rotation signal. Once the system is calibrated, i.e., once k_{rot} is known, Γ^{mag} can be directly measured [28].

[1] J. H. Poynting, Proc. R. Soc. London, Ser. A **82**, 560 (1909).
[2] R. A. Beth, Phys. Rev. **50**, 115 (1936).
[3] N. Carrara, Nuovo Cimento **6**, 50 (1949).
[4] P. J. Allen, Am. J. Phys. **74**, 1185 (1966).
[5] A. Ashkin, J. M. Dziedzic, J. E. Bjorkholm, and S. Chu, Opt. Lett. **11**, 288 (1986).
[6] N. B. Simpson, K. Dholakia, L. Allen, and M. J. Padgett, Opt. Lett. **22**, 52 (1997).
[7] P. L. Marston and J. H. Crichton, Phys. Rev. A **30**, 2508 (1984).
[8] L. Allen, M. W. Beijersbergen, R. J. Spreeuw, and J. P. Woerdman, Phys. Rev. A **45**, 8185 (1992).
[9] M. E. Friese, J. Enger, H. Rubinsztein-Dunlop, and N. R. Heckenberg, Phys. Rev. A **54**, 1593 (1996).
[10] M. E. Friese, T. A. Nieminen, N. R. Heckenberg, and H. Rubinsztein-Dunlop, Opt. Lett. **23**, 1 (1998).
[11] M. E. Friese, T. A. Nieminen, N. R. Heckenberg, and H. Rubinsztein-Dunlop, Nature (London) **394**, 348 (1998).
[12] A. I. Bishop, T. A. Nieminen, N. R. Heckenberg, and H. Rubinsztein-Dunlop, Phys. Rev. A **68**, 033802 (2003).
[13] A. LaPorta and M. D. Wang, Phys. Rev. Lett. **92**, 190801 (2004).
[14] K. Volke-Sepulveda *et al.*, J. Opt. B: Quantum Semiclassical Opt. **4**, S82 (2002).
[15] H. He, M. E. Friese, N. R. Heckenberg, and H. Rubinsztein-Dunlop, Phys. Rev. Lett. **75**, 826 (1995).
[16] E. Santamato, A. Sasso, B. Piccirillo, and A. Vella, Opt. Express **10**, 871 (2002).
[17] S. J. Paddack and John W. Rhee, Geophys. Res. Lett. **2**, 365 (1975).
[18] E. Higurashi, H. Ukita, H. Tanaka, and O. Ohguchi, Appl. Phys. Lett. **64**, 2209 (1994).
[19] P. Galajda and P. Ormos, Appl. Phys. Lett. **78**, 249 (2001).
[20] L. Paterson *et al.*, Science **292**, 912 (2001).
[21] Z.-P. Luo, Y.-L. Sun, and K.-N. An, Appl. Phys. Lett. **76**, 1779 (2000).
[22] K. D. Bonin, B. Kourmanov, and T. G. Walker, Opt. Express **10**, 984 (2002).
[23] A. I. Bishop, T. A. Nieminen, N. R. Heckenberg, and H. Rubinsztein-Dunlop, Phys. Rev. Lett. **92**, 198104 (2004).
[24] M. Capitanio, D. Normanno, and F. S. Pavone, Opt. Lett. **29**, 2231 (2004).

[25] P. Paroli, in *Magnetic Properties of Matter*, edited by F. Borsa and V. Tognetti (World Scientific Publishing Co., Singapore, 1988), pp. 335–368.
[26] M. Capitanio *et al.*, Rev. Sci. Instrum. **73**, 1687 (2002).
[27] L. Sacconi *et al.*, Opt. Lett. **26**, 1359 (2001).
[28] G. Romano, L. Sacconi, M. Capitanio, and F. S. Pavone, Opt. Commun. **215**, 323 (2003).
[29] K. Svoboda, C. F. Schmidt, B. J. Schnapp, and S. M. Block, Nature (London) **365**, 721 (1993).
[30] S. M. Barnett and L. Allen, Opt. Commun. **110**, 670 (1994).
[31] P. Galajda and P. Ormos, Opt. Express **11**, 446 (2003).
[32] Z. Bryant *et al.*, Nature (London) **424**, 338 (2003).
[33] T. R. Strick *et al.*, Science **271**, 1835 (1996).
[34] R. Yasuda *et al.*, Nature (London) **410**, 898 (2001).
[35] F. Amblard, B. Yurke, A. Pargellis, and S. Leibler, Rev. Sci. Instrum. **67**, 818 (1996).
[36] C. Wilhelm, J. Browaeys, A. Ponton, and J.-C. Bacri, Phys. Rev. E **67**, 011504 (2003).
[37] T. R. Strick, J.-F. Allemand, D. Bensimon, and V. Croquette, Biophys. J. **74**, 2016 (1998).
[38] T. R. Strick, V. Croquette, and D. Bensimon, Proc. Natl. Acad. Sci. U.S.A. **95**, 10 579 (1998).
[39] See EPAPS Document No. E-PLRAAN-70-102411 for two movies of two trapped and single beads rotated by a rotating magnetic field. A direct link to this document may be found in the online article's HTML reference section. The document may also be reached via the EPAPS homepage (http://www.aip.org/pubservs/epaps.html) or from ftp.aip.org in the directory/epaps/. See the EPAPS homepage for more information.
[40] Z. L. Liu *et al.*, J. Magn. Magn. Mater. **265**, 98 (2003).
[41] D. Sohn *et al.*, J. Colloid Interface Sci. **177**, 31 (1996).
[42] S. Melle, G. Fuller, and M. A. Rubio, Phys. Rev. E **61**, 4111 (2000).
[43] K. Wormuth, J. Colloid Interface Sci. **241**, 366 (2001).
[44] A. H. Morrison, *The Physical Principles of Magnetism* (John Wiley & Sons Inc., Washington, DC, 1999), p. 333.